Magnesium suppresses defects in the formation of 70S ribosomes as well as in sporulation caused by lack of several individual ribosomal proteins.

Genki Akanuma,[a,b*] Kotaro Yamazaki,[a,] Yuma Yagishi,[a] Yuka Iizuka,[c] Morio Ishizuka,[c] Fujio Kawamura,[a] and Yasuyuki Kato-Yamada.[a,b]

[a]*Department of Life Science, College of Science, Rikkyo University, Toshima-ku, Tokyo 171-8501, Japan*

[b]*Research Center for Life Science, College of Science, Rikkyo University, Toshima-ku, Tokyo 171-8501, Japan*

[c]*Department of Applied Chemistry, Faculty of Science and Engineering, Chuo University, Bunkyo-ku, Tokyo 112-8551, Japan*

Running Head: Mg^{2+} suppresses defects caused by lack of ribosomal proteins

*Corresponding author: Phone & Fax: +81-3-3895-4579**;** E-mail: akanuma@rikkyo.ac.jp,

Keywords: Ribosome, Ribosomal protein, Magnesium, *Bacillus subtilis*

ABSTRACT

Individually, the ribosomal proteins L1, L23, L36 and S6 are not essential for cell proliferation of *B. subtilis*, but the absence of any one of these ribosomal proteins causes a defect in the formation of the 70S ribosomes and a reduced growth rate. In mutant strains individually lacking these ribosomal proteins, the cellular Mg^{2+} content was significantly reduced. The deletion of YhdP, an exporter of Mg^{2+}, and overexpression of MgtE, the main importer of Mg^{2+}, increased the cellular Mg^{2+} content and restored the formation of 70S ribosomes in these mutants. The increase in the cellular Mg^{2+} content improved the growth rate of the Δ*rplA* (L1) and the Δ*rplW* (L23) mutant but did not restore those of the Δ*rpmJ* (L36) and the Δ*rpsF* (S6) mutants. The lack of L1 caused a decrease in the production of Spo0A, the master regulator of sporulation, resulting in a decreased sporulation frequency. However, deletion of *yhdP* and overexpression of *mgtE* increased the production of Spo0A and partially restored the sporulation frequency in the Δ*rplA* (L1) mutant. These results indicate that Mg^{2+} can partly complement the function of several ribosomal proteins, probably by stabilizing the conformation of the ribosome.

IMPORTANCE

We previously reported that an increase in the cellular Mg^{2+} content can suppress defects in 70S ribosome formation and growth rate caused by the absence of ribosomal protein L34. In

the present study, we demonstrated that even in mutants lacking individual ribosomal proteins other than L34 (L1, L23, L36 and S6), an increase in the cellular Mg^{2+} content could restore the 70S ribosome formation. Moreover, the defect in sporulation caused by the absence of L1 was also suppressed by an increase in the cellular Mg^{2+} content. These findings indicate that at least part of the function of these ribosomal proteins can be complemented by Mg^{2+}, which is essential for all living cells.

INTRODUCTION

The bacterial ribosome (70S), which plays a central role in protein synthesis, is a complex macromolecule that is composed of small (30S) subunit and large (50S) subunits. The small subunit is comprised of the 16S rRNA and more than 20 proteins, whereas the large subunit is comprised of the 23S and 5S rRNAs and more than 30 proteins (1, 2). Protein synthesis by the ribosome, called translation, requires the coordinated action of these subunits. The small subunit associates with the mRNA and the anticodon stem-loop of the bound tRNA, and engages in ensuring the fidelity of translation by checking for correct pairing between the codon and anticodon (3-7). The large subunit associates with the acceptor arms of the tRNA and catalyzes the formation of a peptide bond between the amino acid attached to the tRNA in the A-site and the nascent peptide chain bound to the tRNA in the P-site (8, 9). The ribosomal proteins that constitute these subunits play important role(s) in translation. For instance, ribosomal protein L1, which is localized to the stalk region near the E-site (10, 11),

66 plays a critical role in the translocation of the newly deacylated tRNA from the P to the E site
67 (12). Ribosomal protein L2 plays important roles in binding of the tRNA to the A and P sites,
68 peptidyltransferase activity, and formation of the peptide bond (13-17). Therefore, the mature
69 conformation of the 70S ribosomes is required for efficient translation activity. Although the
70 ribosomal proteins are important in the translation processes as well as in the association of
71 the ribosomal subunits (13, 18, 19), several genes encoding ribosomal protein can be deleted.
72 In *Escherichia coli*, 22 of the 54 genes for ribosomal proteins are not individually essential
73 for cell proliferation (20, 21). Similarly, in *Bacillus subtilis*, 22 of the 57 genes for ribosomal
74 proteins can be individually deleted (22). The *rpmH* gene, encoding ribosomal protein L34,
75 which is a component of the large subunit, is one of the nonessential genes. Mutants lacking
76 L34 have a severe defect in the formation of the 70S ribosome and a reduced growth rate
77 (22). However, we found that the defect in the formation of 70S ribosomes and the reduction
78 in the growth late could be suppressed by an increase in the Mg^{2+} content in the cell (23).
79 Magnesium ions are the most abundant divalent cations in living cells (24, 25), and are
80 important for the maintenance of ribosome structure. Mg^{2+} is required for both stabilization
81 of the secondary structure of rRNA and binding of the ribosomal proteins to the rRNA
82 (26-28). The *in vitro* association of the 30S and 50S ribosomal subunits to form intact 70S
83 ribosomes depends strongly on the concentration of Mg^{2+} (29-31). Therefore, we believe that
84 Mg^{2+} can partly complement the L34 function by stabilizing both the conformation of the
85 50S subunit and the intersubunit bridges.

86 In the present study, to elucidate whether Mg^{2+} can also complement mutant strains
87 lacking ribosomal proteins other than L34, we examined the effect of increasing the Mg^{2+}

content in mutant strains individually lacking ribosomal proteins L1, L23, L36 and S6 on the formation of 70S ribosomes, the growth rate, and on sporulation.

RESULTS

Reduction in the cellular Mg^{2+} content caused by lack of ribosomal proteins was restored by disruption of *yhdP* and overexpression of *mgtE*.

The defect in the formation of 70S ribosomes caused by the absence of L34 could be suppressed by increasing the cellular Mg^{2+} content (23). To investigate the generality of the partial complementation of the ribosomal-protein function by Mg^{2+}, a disruption of *yhdP* and the multicopy plasmid pDGmgtE, which can induce the overexpression of *mgtE*, were introduced into mutants lacking individual ribosomal proteins L1, L23, L36 and S6. MgtE is the main importer of Mg^{2+} (32), whereas YhdP is probably an exporter of Mg^{2+} in *B. subtilis* (23). We previously reported that the absence of L34 (RpmH) caused a decrease in the Mg^{2+} content in the cell, probably due to a reduced number of 70S ribosomes, and that the Mg^{2+} content in the Δ*rpmH* mutant was restored by disruption of *yhdP* and overexpression of *mgtE* (23). Similarly, the Mg^{2+} contents in the Δ*rplA* (L1), Δ*rplW* (L23) and Δ*rpmJ* (L36) mutants were also significantly reduced (Fig. 1). However, the Mg^{2+} content in these three mutants was restored, albeit incompletely, by disruption of *yhdP* and overexpression of *mgtE* (Fig. 1). In this experiment, the cellular Mg^{2+} concentration was calculated by dividing the amount of Mg^{2+} per cell by the cell volume. The cell volume of each mutant was estimated from the cell

size, which was measured by microscopic analysis, as described in Materials and Methods. However, the cell size of the Δ*rpsF* (S6) mutant could not be defined, because the cellular morphology of the Δ*rpsF* mutant was aberrantly filamentous (Fig. S1). Thus, in the Δ*rpsF* mutant, the relative Mg^{2+} amount per cell, when the Mg^{2+} amount of a cell in the parental strain was defined as 1, is shown in Fig. 1. Although a comparison of the Mg^{2+} content in the Δ*rpsF* mutants with that in the wild type was difficult, the Mg^{2+} content in the Δ*rpsF* mutants was certainly increased by disruption of *yhdP* and overexpression of *mgtE*. It should be noted that the Mg^{2+} ions that were chelated in ribosomes and other enzymes were also detected by this method, because the cells were completely disrupted by sonication and proteins were denatured by acid treatment.

The effect of increasing the cellular Mg^{2+} content of mutants lacking individual ribosomal proteins on the formation of 70S ribosomes and the growth rate.

As shown in Fig. 2, the lack of individual ribosomal proteins (L1, L23, L36, S6) caused defects in the formation of 70S ribosomes that are consistent with our previous data (22). The defect in 70S-ribosome formation observed in these mutants was suppressed by disruption of *yhdP* and overexpression of *mgtE*, to varying degrees (Fig. 2). In all of the mutants investigated here, the amount of 70S ribosomes relative to the amount of dissociated subunits was restored by increasing the Mg^{2+} content in the cell. These results indicate that Mg^{2+} can suppress the defect in the formation of 70S ribosomes caused by the absence of several individual ribosomal proteins.

We next investigated the effect of the cellular Mg^{2+} content on the growth rate of the

mutants. We have reported that the slow growth observed in the Δ*rpmH* (L34) mutant was suppressed by an increase in the Mg^{2+} content, probably due to the restoration of the amount of 70S ribosomes (23). A reduction in the growth rate was observed in the mutants lacking individual ribosomal proteins, which agrees with our previous results (22). As expected, in the Δ*rplA* (L1) and Δ*rplW* (L23) mutants, the growth rate was partially restored by disruption of *yhdP* and overexpression of *mgtE* (Fig. 3A and B, Table 1). When only *mgtE* was overexpressed in the Δ*rplA* (L1) mutant, its effect on the growth rate was minimal (23). The combination of overexpression of *mgtE* and disruption of *yhdP*, however, increased the growth rate of the Δ*rplA* (L1) mutant. In contrast, the growth rates of the Δ*rpmJ* (L36) and Δ*rpsF* (S6) mutants were not significantly increased when the cellular Mg^{2+} content was increased (Fig. 3C and D, Table 1). Therefore, the increased formation of 70S ribosomes did not necessarily restore the growth rate of the mutants lacking individual ribosomal proteins.

The increase in the cellular Mg^{2+} content suppresses the defect in sporulation caused by the absence of ribosomal protein L1.

We previously found that the absence of ribosomal protein L1 causes a defect in sporulation (22). It should be note that this phenotype was not caused solely by the decreased growth rate, because the sporulation frequency of the Δ*rpmH* mutant, which also showed a severe growth defect similar to that of the Δ*rplA* (L1) mutant, was almost the same as that of the wild type (22). We therefore investigated whether the sporulation defect of the Δ*rplA* (L1) mutant could be suppressed by Mg^{2+}. Consistent with our previous data, the Δ*rplA* (L1)

153 mutant was severely defective in forming heat-resistant spores (the sporulation frequency
154 was less than 0.01%) (Table 2). However, the sporulation frequency of the Δ*rplA* (L1) mutant
155 was significantly restored by disruption of *yhdP* and overexpression of *mgtE* (Table 2). In
156 addition, the growth rate of the Δ*rplA* (L1) mutant in sporulation medium was also restored
157 by disruption of *yhdP* and overexpression of *mgtE* (Fig. 4A). These results indicate that
158 increasing the cellular Mg^{2+} content can suppress not only the growth defect, but also the
159 sporulation defect in the Δ*rplA* (L1) mutant.

160 The restoration of spore formation by the Δ*rplA* (L1) mutant prompted us to identify
161 which stage of sporulation was affected by the absence of L1 and restoration by Mg^{2+}. At the
162 initiation stage of *B. subtilis* sporulation, cells divide asymmetrically, and chromosomal
163 DNA is concentrated in the forespore (33). In fact, asymmetric septation and concentration of
164 chromosomal DNA were detected in the wild-type cells five h after inoculation in sporulation
165 medium (Fig. S2). In contrast, in the Δ*rplA* (L1) cells, asymmetric septation was not
166 observed even 24 h after inoculation (Fig. S2). However, the disruption of *yhdP* and
167 overexpression of *mgtE* helped formation of the asymmetric septum in the Δ*rplA* (L1) cells
168 (Fig. S2). We next examined the level of Spo0A in the Δ*rplA* (L1) mutant. Phosphorylation of
169 Spo0A, the master transcriptional regulator of sporulation, governs the decision to initiate
170 sporulation (34-36).In wild-type cells, the level of Spo0A increased four hours after
171 inoculation into sporulation medium, whereas Spo0A was barely detectible in Δ*rplA* (L1)
172 cells even 10 h after inoculation (Fig. 4B). The disruption of *yhdP* and overexpression of
173 *mgtE* in the Δ*rplA* (L1) cells increased the amount of Spo0A by 9 h after inoculation,

174 although the level of Spo0A remained lower than that in wild type (Fig. 4B). These results
175 indicate that the defect in the initiation stage of sporulation caused by the absence of L1 can
176 be at least partially suppressed by an increase in the Mg^{2+} content in the cell.
177
178
179 **DISCUSSION**
180
181 The cellular Mg^{2+} contents of the mutant strains individually lacking L1, L23, or L36 were
182 reduced compared to that of wild type, while that of the Δ*rpsF* (S6) mutant was difficult to
183 calculate because of its filamentous cellular morphology (Fig. 1 and Fig. S1). The reduction
184 in the amount of Mg^{2+} was probably caused by the lower amount of 70S ribosomes, which
185 harbor more than 170 Mg^{2+} ions per complex (37), and by a decrease in the amount of protein
186 and RNA other than ribosomes that can chelate Mg^{2+}. In fact, we previously showed that the
187 reduction in the cellular Mg^{2+} content correlated with the decrease in the amount of 70S
188 ribosomes (23). On the other hand, the disruption of *yhdP* and overexpression of *mgtE*
189 increased cellular Mg^{2+} content and restored the formation of 70S ribosomes in the mutants
190 lacking individual ribosomal proteins tested here (Fig. 2). Although the absence of L34
191 causes ribosomal protein L16 to dissociate from the 50S subunit, the increase in the Mg^{2+}
192 content restores the binding of L16 to the 50S subunit, indicating that Mg^{2+} can stabilize the
193 conformation of 50S subunits lacking L34 (23). Likewise, stabilization of the conformation
194 of each subunit as well as inter bridges between the subunits by Mg^{2+} probably restored 70S
195 formation in the mutants lacking individual ribosomal proteins tested here (L1, L23, L36 and

196 S6).

197 The increase in the 70S ribosome formation restored cellular translational activity that
198 may have resulted in the suppression of the defect in the growth rate of the Δ*rplA* (L1) and
199 Δ*rplW* (L23) mutants (Fig. 3 and Table 1). However, the restoration of growth rate of these
200 mutants was only partial. Possible reasons for this partial restoration of the growth are (i) an
201 incomplete restoration of the normal amount of 70S ribosomes, and (ii) functions of the
202 ribosomal proteins other than in stabilizing the 70S ribosomes could not be complemented by
203 Mg^{2+}. Ribosomal protein L1 plays a critical role in the translocation of the newly deacylated
204 tRNA from the P to the E site (12), while ribosomal protein L23, which is located at the
205 polypeptide exit channel of the large subunit, tethers trigger factor to the ribosome (38).
206 Trigger factor, which is the first molecular chaperone interacting with newly synthesized
207 polypeptides by the ribosome, promotes protein folding (39-41). The functions of these
208 ribosomal proteins are probably essential for efficient growth. In contrast to mutants lacking
209 L1 or L23, the growth rates of the Δ*rpmJ* (L36) and Δ*rpsF* (S6) mutants were not
210 significantly increased when the Mg^{2+} content was increased, although 70S ribosome
211 formation was restored to near wild-type levels (Fig. 2 and Fig. 3). Although the detailed
212 functions of L36 and S6 in protein synthesis are unknown, their role(s) in translation or other
213 function(s) do not appear to be complemented by Mg^{2+}. In addition, the filamentous
214 morphology of cells caused by the absence of S6 was not repaired by increasing the cellular
215 Mg^{2+} content.

216 The increase in the cellular Mg^{2+} content suppressed the defect not only of 70S ribosome
217 formation, but also the sporulation defect of the Δ*rplA* (L1) mutant (Table 2). Although

Spo0A, the master regulator of sporulation, was undetectable in the Δ*rplA* (L1) mutant, Spo0A was clearly produced when the cellular Mg^{2+} content was increased (Fig. 4), and resulted in the restoration of sporulation frequency of the Δ*rplA* (L1) mutant. The phosphorylated form of Spo0A activates expression of sporulation genes as well as its own gene via a positive feedback loop (42). Phosphorylation of Spo0A is achieved by a multicomponent phosphorelay involving at least three kinases called KinA, KinB, and KinC (33, 35). KinA and KinB phosphorylate Spo0F, and phosphorylated Spo0F transfers the phosphoryl group to Spo0B. Finally, Spo0A receives a phosphoryl group from phosphorylated Spo0B (43). In addition, KinC can directly phosphorylate Spo0A without the Spo0F and Spo0B phosphorelay (33). Inversely, phosphorylated Spo0F and Spo0A can be dephosphorylated by phosphatases such as Spo0E (33). It is likely that an inhibition of the multicomponent phosphorelay, and/or the dephosphorylation of Spo0F and Spo0A by the phosphatases was caused by the lack of L1, and it could be suppressed by an increase in the Mg^{2+} content. The improved Spo0A activation in the Δ*rplA* (L1) mutant by Mg^{2+} was probably not due to the complementation of an extraribosomal function of L1, but to restoration of the amount of 70S ribosomes and/or an increase in the cellular translational activity.

In the present study, we demonstrated that the defect in the formation of 70S ribosomes as well as in the sporulation caused by lack of individual ribosomal proteins can be suppressed by increasing the cellular Mg^{2+} content. Mg^{2+} plays a crucial role not only in the ribosome but also in numerous biological processes and cellular functions, such as the activation and catalytic reactions of hundreds of enzymes, utilization of ATP, and maintenance of genomic

stability (44, 45). Clarifying the relationship between the ribosome and Mg^{2+}, both of which are essential to living cells, is important for understanding cellular function. It has been suggested that the sizes of ribosomal proteins have increased during evolution to complement the function of the rRNA, which originally acted as a ribozyme (46, 47). From another point of view, increasing of the sizes of ribosomal proteins and/or binding of ribosomal proteins to the ribosome during evolution can be considered to complement the Mg^{2+} function in the ribosome, because in the ribosome, the relative abundance of Mg^{2+} is decreased whereas that of ribosomal proteins is increased (47, 48). Further investigation to reveal the mechanism of complementation of the ribosomal-protein function by Mg^{2+} may provide important information about the evolution of the ribosome.

MATERIALS AND METHODS

Media and culture conditions. LB medium (49), LB agar, and 2×Schaeffer's sporulation medium supplemented with 0.1% glucose (2×SG) (50) were used. The culture conditions and media for preparing competent cells have been described previously (51). When required, 5 μg ml^{-1} chloramphenicol, 5 μg ml^{-1} kanamycin and 1 mM isopropyl-β-D-thiogalactopyranoside (IPTG) were added to the media. Growth curves of *B. subtilis* cells were generated by automatically measuring the OD_{660} value of each culture every 5 min using a TVS062CA incubator (ADVANTEC).

Bacterial strains. All of the *B. subtilis* strains used in this study were isogenic with *B.*

subtilis strain 168 *trpC2*. The Δ*rplA*::*cat*, Δ*rplW*::*cat*, Δ*rpmJ*::*cat* and Δ*rpsF*::*cat* strains, which were constructed by replacing the open reading frame of each gene with a promoterless *cat* gene lacking a Rho-independent terminator sequence, were described previously (22). Chromosomal DNA extracted from the Δ*rplA*::*cat*, Δ*rplW*::*cat*, Δ*rpmJ*::*cat* and Δ*rpsF*::*cat* was used to transform the strain harboring Δ*yhdP*::*erm* and the plasmid pDGmgtE, which carries the *mgtE* gene under the control of an IPTG-inducible Pspac promoter (23), and the transformants were selected on the basis of their chloramphenicol-resistant phenotype.

Measurement of the cellular Mg^{2+} content. The cellular Mg^{2+} content was measured as described previously (23). Briefly, *B. subtilis* cells were grown in LB medium to exponential phase and harvested. Simultaneously, viable cells were counted by plating the culture on LB agar plates. The cells were resuspended in lysis buffer and disrupted by sonication, and then the pH of the crude extract was adjusted to approximately 3.0 with hydrochloric acid in order to denature the proteins. The amount of Mg^{2+} in the cell lysate was measured with a Metallo Assay Kit for magnesium (Metallogenics). The Mg^{2+} content per cell was calculated by dividing the amount of Mg^{2+} in the crude extract by the number of viable cells. The concentration of Mg^{2+} was calculated by assuming that a *B. subtilis* cell is a cylinder. To measure the cell size (radius and length), microscopic images were analyzed by MicrobeJ, an ImageJ plug-in (52). The mean size of >30 cells was used for the calculation.

Sucrose density gradient sedimentation analysis. *B. subtilis* cells were grown in LB medium at 37°C with shaking to exponential phase (OD_{600} ~0.4) and harvested. The sucrose density gradient sedimentation analysis was performed as described previously (22). Briefly,

284 the cells were disrupted by passage through a French pressure cell and cell debris was
285 removed by centrifugation. Aliquots of extract were layered onto 10–40% sucrose density
286 gradients, which were subjected to centrifugation at 4°C for 17.5 h at 65,000 ×*g* (Hitachi
287 P40ST rotor). Samples were collected with a Piston Gradient Fractionator (BioComP), and
288 absorbance profiles were monitored at 254 nm using a Bio-Mini UV Monitor (ATTO, Japan).
289 When normalizing the applied volume by the total absorbance at 260 nm, 10 A_{260} units of
290 crude extract per tube were used.

291 **Sporulation assay.** *B. subtilis* cells were grown in 2× SG medium for 24 h at 37°C with
292 shaking. Heat-resistant spores were counted by heating the cells at 80°C for 10 min, plating
293 them on LB agar plates, and then incubating the plates at 37°C for 24 h.

294 **Microscopic imaging.** *B. subtilis* cells were grown in 2× SG medium at 37°C with
295 shaking. At the indicated times, 500 µl of the culture was removed and subjected to
296 centrifugation at 12,000 × g for 1 min. The cell pellet was resuspended in 40 µl of culture
297 supernatant and then FM4-64 (Invitrogen) and DAPI (Wako Pure Chemical Industries) were
298 added to final concentrations of 10 µg/ml and 5 µg/ml, respectively. The cell suspension was
299 mounted on a microscope slide, coated with poly-L-lysine to fix the cells, and differential
300 interference contrast and fluorescence images were obtained with a LSM800, a confocal
301 fluorescence microscope (Carl Zeiss).

302 **Western blot analysis.** Western blot analysis was performed according to a previously
303 described method (53). Aliquots (15 µg of protein) of crude cell extracts were loaded onto a
304 sodium dodecyl sulfate polyacrylamide gel (12%) and transferred to a PVDF membrane
305 (Millipore Co., Japan). This membrane was then used in the Western blot assay using antisera

306 (1:10,000 dilution) against Spo0A (54).

307

308 **ACKNOWLEDGEMENTS**

309 This work was supported in parts by Grants-in-Aid for Scientific Research (C) (26450101
310 and 15K07013 to G. A. and Y. K.-Y., respectively), Grant-in-Aid for Young Scientists (B)
311 (17K15253 and 23770157 to G. A. and Y. K.-Y., respectively) and Strategic Research
312 Foundation Grant-aided Project for Private Universities (S1201003 to F. K. and Y. K.-Y.)
313 from the Ministry of Education, Culture, Sports, Science, and Technology of Japan.

REFERENCES

1. Kurland CG. 1972. Structure and function of the bacterial ribosome. Annu. Rev. Biochem. **41:**377–408.

2. Nomura M. 1970. Bacterial ribosome. Bacteriol. Rev. **34:**228–277.

3. Jenner L, Demeshkina N, Yusupova G, Yusupov M. 2010. Structural rearrangements of the ribosome at the tRNA proofreading step. Nat. Struct. Mol. Biol. **17**:1072–1078.

4. Ogle JM, Brodersen DE, Clemons WM Jr, Tarry MJ, Carter AP, Ramakrishnan V. 2001. Recognition of cognate transfer RNA by the 30S ribosomal subunit. Science 292:897–902.

5. Schluenzen F, Tocilj A, Zarivach R, Harms J, Gluehmann M, Janell D, Bashan A, Bartels H, Agmon I, Franceschi F, Yonath A. 2000. Structure of functionally activated small ribosomal subunit at 3.3 Å resolution. Cell 102:615–623.

6. Wimberly BT, Brodersen DE, Clemons WM Jr, Morgan-Warren RJ, Carter AP, Vonrhein C, Hartsch T, Ramakrishnan V. 2000 Structure of the 30S ribosomal subunit. Nature 407:327–339.

7. Yusupova GZ, Yusupov MM, Cate JH, Noller HF. 2001. The path of messenger RNA through the ribosome. Cell 106:233–241.

8. Ban N, Nissen P, Hansen J, Moore PB, Steitz TA. 2000. The complete atomic structure of the large ribosomal subunit at 2.4 Å resolution. Science 289:905–920.

9. Nissen P, Hansen J, Ban N, Moore PB, Steitz TA. 2000. The structural basis of ribosome activity in peptide bond synthesis. Science. 289:920–930.

10. Yusupov MM, Yusupova GZ, Baucom A, Lieberman K, Earnest TN, Cate JH,

Noller HF. 2001. Crystal structure of the ribosome at 5.5 Å resolution. Science **292:**883–896.

11. Agrawal RK, Lata RK, Frank J. 1999. Conformational variability in *Escherichia coli* 70S ribosome as revealed by 3D cryo-electron microscopy. Int. J. Biochem. Cell. Biol. **31:**243–254.

12. Fei J, Kosuri P, MacDougall DD, Gonzalez RL. 2008. Coupling of ribosomal L1 stalk and tRNA dynamics during translation elongation. Mol. Cell 30:348–359.

13. Diedrich G, Spahn CM, Stelzl U, Schafer MA, Wooten T, Bochkariov DE, Cooperman BS, Traut RR, Nierhaus KH. 2000. Ribosomal protein L2 is involved in the association of the ribosomal subunits, tRNA binding to A and P sites and peptidyl transfer. EMBO J. **19:**5241–5250.

14. Khaitovich P, Mankin AS, Green R, Lancaster L, Noller HF. 1999. Characterization of functionally active subribosomal particles from *Thermus aquaticus*. Proc. Natl. Acad. Sci. USA **96:**85–90.

15. Schulze H, Nierhaus KH. 1982. Minimal set of ribosomal components for reconstitution of the peptidyltransferase activity. EMBO J. **1:**609–613.

16. Uhlein M, Weglöhner W, Urlaub H, Wittmann-Liebold B. 1998. Functional implications of ribosomal protein L2 in protein biosynthesis as shown by *in vivo* replacement studies. Biochem. J. **331:**423–430.

17. Willumeit R, Forthmann S, Beckmann J, Diedrich G, Ratering R, Stuhrmann HB, Nierhaus KH. 2001. Localization of the protein L2 in the 50S subunit and the 70S *E. coli* ribosome. J. Mol. Biol. **305:**167–177.

358 **18. Teraoka H, Nierhaus KH.** 1978. Protein L16 induces a conformational change when
359 incorporated into a L16-deficient core derived from *Escherichia coli* ribosomes. FEBS
360 Lett. **88:**223–226.
361 **19. Suzuki S, Tanigawa O, Akanuma G, Nanamiya H, Kawamura F, Tagami K,**
362 **Nomura N, Kawabata T, Sekine Y.** 2014. Enhanced expression of *Bacillus subtilis*
363 *yaaA* can restore both the growth and sporulation defects caused by mutation of *rplB*,
364 encoding ribosomal protein L2. Microbiology **160:**1040–1053.
365 **20. Baba T, Ara T, Hasegawa M, Takai Y, Okumura Y, Baba M, Datsenko KA, Tomita**
366 **M, Wanner BL, Mori H.** 2006. Construction of *Escherichia coli* K-12 in-frame,
367 single-gene knockout mutants: the Keio collection. Mol. Syst. Biol. 2: 2006.0008.
368 **21. Shoji S, Dambacher CM, Shajani Z, Williamson JR, Schultz PG.** 2011. Systematic
369 chromosomal deletion of bacterial ribosomal protein genes. J. Mol. Biol. **413:**751–761.
370 **22. Akanuma G, Nanamiya H, Natori Y, Yano K, Suzuki S, Omata S, Ishizuka M,**
371 **Sekine Y, Kawamura F.** 2012. Inactivation of ribosomal protein genes in *Bacillus*
372 *subtilis* reveals importance of each ribosomal protein for cell proliferation and cell
373 differentiation. J. Bacteriol. **194:**6282–6291.
374 **23. Akanuma G, Kobayashi A, Suzuki S, Kawamura F, Shiwa Y, Watanabe S,**
375 **Yoshikawa H, Hanai R, Ishizuka M.** 2014. Defect in the formation of 70S ribosomes
376 caused by lack of ribosomal protein L34 can be suppressed by magnesium. J Bacteriol.
377 **196**:3820–3830.
378 **24. Maguire ME, Cowan JA.** 2002. Magnesium chemistry and biochemistry. Biometals **15**:
379 203–210.

380 **25. Wacker WE.** 1969. The biochemistry of magnesium. Ann. N Y Acad. Sci. **162**: 717–726.

381 **26. Drygin D, Zimmermann RA.** 2000. Magnesium ions mediate contacts between
382 phosphoryl oxygens at positions 2122 and 2176 of the 23S rRNA and ribosomal protein
383 L1. RNA **6:**1714–1726.

384 **27. Klein DJ, Moore PB, Steitz TA.** 2004. The contribution of metal ions to the structural
385 stability of the large ribosomal subunit. RNA **10:**1366–1379.

386 **28. Petrov AS, Bernier CR, Hsiao C, Okafor CD, Tannenbaum E, Stern J, Gaucher E,**
387 **Schneider D, Hud NV, Harvey SC, Williams LD.** 2012. RNA-magnesium-protein
388 interactions in large ribosomal subunit. J. Phys. Chem. B. **116:**8113–8120.

389 **29. Blaha G, Burkhardt N, Nierhaus KH.** 2002. Formation of 70S ribosomes: large
390 activation energy is required for the adaptation of exclusively the small ribosomal
391 subunit. Biophys. Chem. **96:**153–161.

392 **30. Liiv A, O'Connor M.** 2006. Mutations in the intersubunit bridge regions of 23 S rRNA.
393 J. Biol. Chem. **281:**29850–29862.

394 **31. Tissieres A, Watson JD, Schlessinger D, Hollingworth BR.** 1959. Ribonucleoprotein
395 particles from *Escherichia coli*. J. Mol. Biol. **1:**221–233.

396 **32. Wakeman CA, Goodson JR, Zacharia VM, Winkler WC.** 2014. Assessment of the
397 Requirements for Magnesium Transporters in *Bacillus subtilis*. J. Bacteriol. **196:**1206–
398 1214.

399 **33. Higgins D, Dworkin J.** 2012 Recent progress in *Bacillus subtilis* sporulation. FEMS
400 Microbiol. Rev. 36:131–148.

401 **34. Hoch JA.** 1993. Regulation of the phosphorelay and the initiation of sporulation in

Bacillus subtilis. Annu. Rev. Microbiol. **47**:441–465.

35. Stephenson K, Hoch JA. 2002. Evolution of signalling in the sporulation phosphorelay. Mol. Microbiol. **46**:297–304.

36. Molle V, Fujita M, Jensen ST, Eichenberger P, Gonzalez-Pastor JE, Liu JS, Losick R. 2003. The Spo0A regulon of *Bacillus subtilis*. Mol. Microbiol. **50**:1683–1701.

37. Schuwirth BS, Borovinskaya MA, Hau CW, Zhang W, Vila-Sanjurjo A, Holton JM, Cate JH. 2005. Structures of the bacterial ribosome at 3.5 A resolution. Science **310:**827–834.

38. Kramer G, Rauch T, Rist W, Vorderwulbecke S, Patzelt H, Schulze-Specking A, Ban N, Deuerling E, Bukau B. 2002. L23 protein functions as a chaperone docking site on the ribosome. Nature **419**:171–174.

39. Merz F, Boehringer D, Schaffitzel C, Preissler S, Hoffmann A, Maier T, Rutkowska A, Lozza J, Ban N, Bukau B, Deuerling E. 2008. Molecular mechanism and structure of trigger factor bound to the translating ribosome. EMBO J. **27**:1622–1632.

40. Hartl FU, Hayer-Hartl M. 2009. Converging concepts of protein folding *in vitro* and *in vivo*. Nat. Struct. Mol. Biol. **16**:574–581.

41. Hoffmann A, Bukau B, Kramer G. 2010. Structure and function of the molecular chaperone Trigger Factor. Biochim. Biophys. Acta. 1803(6):650–661.

42. Hoch JA. 1991. *spo0* genes, the phosphorelay, and the initiation of sporulation. In *Bacillus subtilis* and other Grampositive bacteria: Biochemistry, physiology, and molecular genetics (eds. A.L. Sonenshein et al.), pp. 747–755. American Society for Microbiology, Washington, D.C

424 **43. Burbulys D, Trach KA, Hoch JA.** 1991 Initiation of sporulation in *B. subtilis* is
425 controlled by a multicomponent phosphorelay. Cell **64**:545–552.
426 **44. Cowan JA.** 2002. Structural and catalytic chemistry of magnesium dependent enzymes.
427 Biometals **15:**225–235
428 **45. Hartwig A.** 2001. Role of magnesium in genomic stability. Mutat. Res. **475:**113–121.
429 **46. Bokov K, Steinberg SV.** 2009. A hierarchical model for evolution of 23S ribosomal
430 RNA. Nature **457**:977–980.
431 **47. Wachowius F, Attwater J, Holliger P.** 2017. Nucleic acids: function and potential for
432 abiogenesis. Q. Rev. Biophys. 50:e4. doi: 10.1017/S0033583517000038.
433 **48. Hsiao C, Mohan S, Kalahar BK, Williams L D.** 2009. Peeling the onion: ribosomes are
434 ancient molecular fossils. Molecular Biology and Evolution **26**:2415–2425.
435 **49. Sambrook J, Fritsch EF, Maniatis T.** 1989. Molecular Cloning: A Laboratory Manual,
436 2nd ed., Cold Spring Harbor Laboratory Press, Cold Spring Harbor, NY.
437 **50. Leighton TJ, Doi RH.** 1971. The stability of messenger ribonucleic acid during
438 sporulation in *Bacillus subtilis*. J. Biol. Chem. **246**:3189 –3195.
439 **51. Ashikaga S, Nanamiya H, Ohashi Y, Kawamura F.** 2000. Natural genetic competence
440 in *Bacillus subtilis* natto OK2. J. Bacteriol. **182:**2411–2415.
441 **52. Jiang C, Brown PJ, Ducret A, Brun YV.** 2014. Sequential evolution of bacterial
442 morphology by co-option of a developmental regulator. Nature **506**:489–493.
443 **53. Nanamiya H, Shiomi E, Ogura M, Tanaka T, Asai K, Kawamura F.** 2003.
444 Involvement of ClpX protein in the post-transcriptional regulation of a competence
445 specific transcription factor, ComK protein, of *Bacillus subtilis*. J Boichem (Tokyo) **133**:

295–302.

54. Nanamiya H, Ohashi Y, Asai K, Moriya S, Ogasawara N, Fujita M, Sadaie Y, Kawamura F. 1998. ClpC regulates the fate of a sporulation initiation sigma factor, σH protein, in *Bacillus subtilis* at elevated temperatures. Mol. Microbiol. **29**:505–513.

Figure legends

Fig. 1. Reduction in the Mg^{2+} content in mutant strains lacking individual ribosomal proteins and partial restoration by disruption of *yhdP* and overexpression of *mgtE*. The Mg^{2+} content per cell in exponential phase, which was measured as described in the Materials and Methods, is shown. In the case of the Δ*rpsF* (S6) mutant, the relative amount of Mg^{2+} per cell is shown (see text for details). White bars indicate the wild type and each mutant lacking individual ribosomal proteins. Gray bars indicate the results when *yhdP* was disrupted and *mgtE* was overexpressed. The means of three independent experiments are shown. Error bars indicate standard deviations.

Fig. 2. Defect in 70S ribosome formation in the absence of each ribosomal protein and its suppression by the disruption of *yhdP* and overexpression of *mgtE*. Crude cell extracts were sedimented through a 10–40% sucrose gradient as described in the Materials and Methods. The 30S, 50S, and 70S peaks are indicated in each individual profile. The term '/ pDGmgtE' indicates the overexpression of *mgtE* in the mutant cells.

Fig. 3. Effects of the increase in cellular Mg^{2+} content on the growth rate of the mutant strains lacking individual ribosomal proteins. Cells were grown in LB at 37°C, and the optical density at 660 nm was measured. Growth curves of wild type and each mutant lacking individual ribosomal proteins are shown using black solid lines and gray solid lines, respectively. Growth curves of each mutant in which *yhdP* was disrupted and *mgtE* was

473 overexpressed are shown by gray dotted lines.

474

475 **Fig. 4.** Reduction in the growth rate and in the production of Spo0A caused by lack of L1 and
476 their suppression by the disruption of *yhdP* and overexpression of *mgtE*. (A) Cells were
477 grown in sporulation medium (2×SG) at 37°C, and the optical density at 660 nm was
478 measured. Growth curves of wild type and the Δ*rplA* (L1) mutant are shown using black and
479 gray solid lines, respectively. The growth curve of the L1 mutant in which *yhdP* was
480 disrupted and *mgtE* was overexpressed is shown by a gray dotted line. (B) Cells were grown
481 in sporulation medium at 37°C, and were collected at the indicated times. Crude cell extracts
482 were subjected to western blot analysis using antisera against the Spo0A. The term '/
483 pDGmgtE' indicates the overexpression of *mgtE* in the mutant cells.

Table 1. Doubling times (min) of mutants lacking ribosomal proteins.

Strain	Parental	Δ*yhdP*/pDGmgtE
wt	21.4 ± 1.4	
Δ*rplA* (L1)	67.7 ± 1.7	54.6 ± 0.49
Δ*rplW* (L23)	56.7 ± 1.9	37.0 ± 2.4
Δ*rpmJ* (L36)	43.3 ± 1.3	41.2 ± 0.54
Δ*rpsF* (S6)	38.2 ± 1.1	36.4 ± 0.49

Means of three independent experiments with ± SD are shown.

Table 2. Restoration of sporulation frequency of the ΔL1 mutant by Mg^{2+}

Strain	C.f.u. ml^{-1*}		Frequency (%)*
	Total	Spores	
wt	6.4×10^8	5.8×10^8	90 ± 7.9
ΔL1	1.6×10^8	2.3×10^2	$1.7 (\pm 1.2) \times 10^{-4}$
ΔL1 Δ*yhdP* / pDGmgtE	3.1×10^8	7.5×10^7	25 ± 4.7

*Means of three independent experiments (± SD for sporulation frequency).

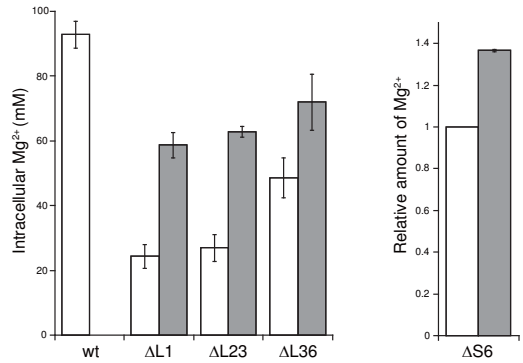

Fig. 1. Reduction in the Mg^{2+} content in mutant strains lacking individual ribosomal proteins and partial restoration by disruption of *yhdP* and overexpression of *mgtE*. The Mg^{2+} content per cell in exponential phase, which was measured as described in the Materials and Methods, is shown. In the case of the Δ*rpsF* (S6) mutant, the relative amount of Mg^{2+} per cell is shown (see text for details). White bars indicate the wild type and each mutant lacking individual ribosomal proteins. Gray bars indicate the results when *yhdP* was disrupted and *mgtE* was overexpressed. The means of three independent experiments are shown. Error bars indicate standard deviations.

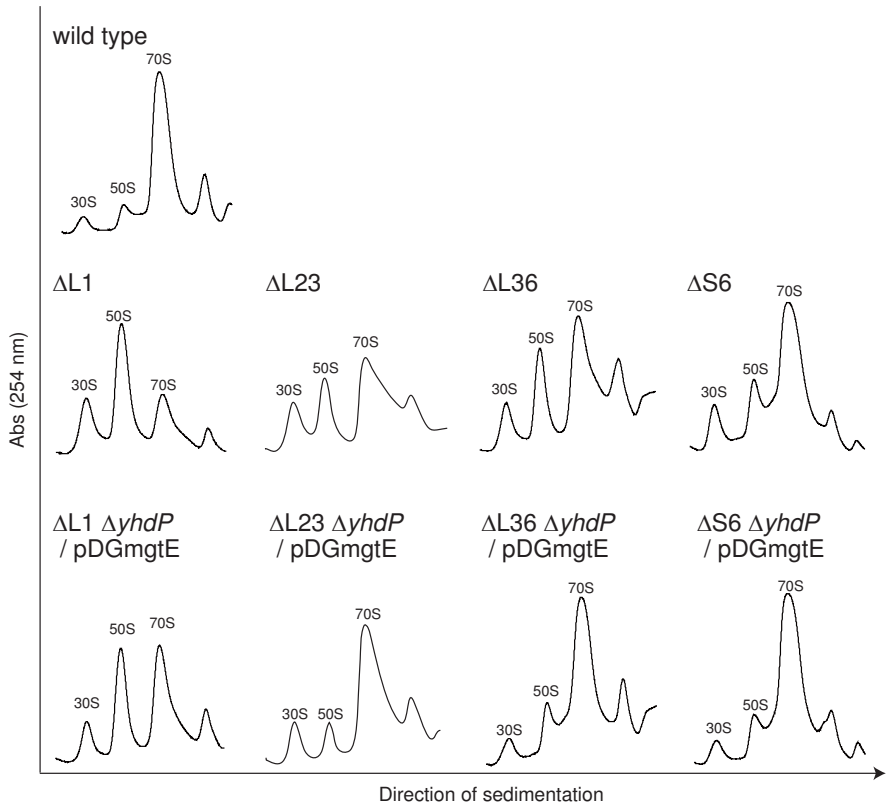

Fig. 2. Defect in 70S ribosome formation in the absence of each ribosomal protein and its suppression by the disruption of *yhdP* and overexpression of *mgtE*. Crude cell extracts were sedimented through a 10–40% sucrose gradient as described in the Materials and Methods. The 30S, 50S, and 70S peaks are indicated in each individual profile. The term '/ pDGmgtE' indicates the overexpression of *mgtE* in the mutant cells.

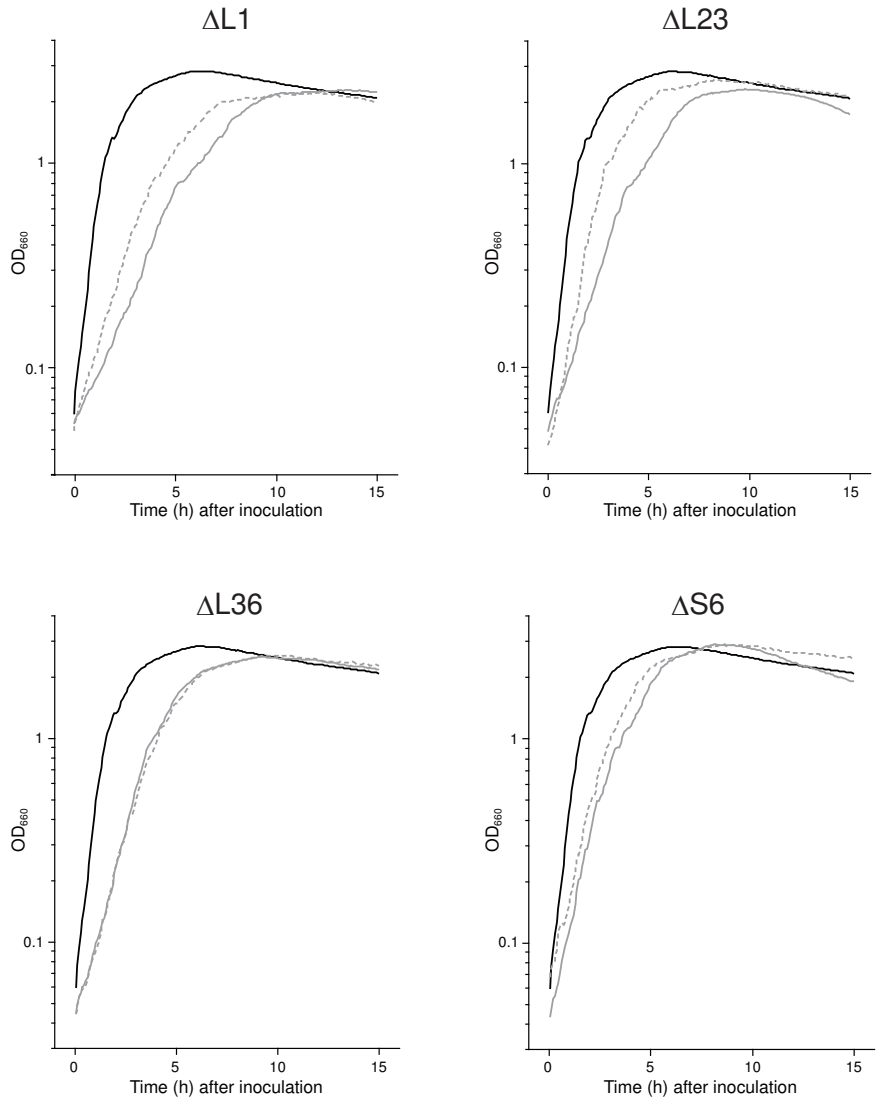

Fig. 3. Effects of the increase in cellular Mg^{2+} content on the growth rate of the mutant strains lacking individual ribosomal proteins. Cells were grown in LB at 37°C, and the optical density at 660 nm was measured. Growth curves of wild type and each mutant lacking individual ribosomal proteins are shown using black solid lines and gray solid lines, respectively. Growth curves of each mutant in which *yhdP* was disrupted and *mgtE* was overexpressed are shown by gray dotted lines.

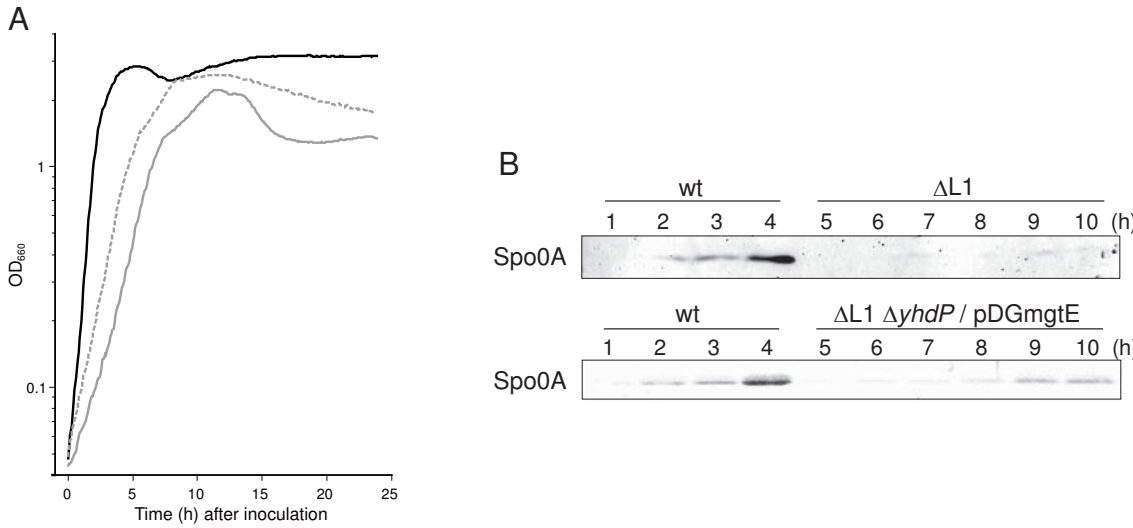

Fig. 4. Reduction in the growth rate and in the production of Spo0A caused by lack of L1 and their suppression by the disruption of *yhdP* and overexpression of *mgtE*. (A) Cells were grown in sporulation medium (2×SG) at 37°C, and the optical density at 660 nm was measured. Growth curves of wild type and the Δ*rplA* (L1) mutant are shown using black and gray solid lines, respectively. The growth curve of the L1 mutant in which *yhdP* was disrupted and *mgtE* was overexpressed is shown by a gray dotted line. (B) Cells were grown in sporulation medium at 37°C, and were collected at the indicated times. Crude cell extracts were subjected to western blot analysis using antisera against the Spo0A. The term '/ pDGmgtE' indicates the overexpression of *mgtE* in the mutant cells.